Proceedings World Geothermal Congress 2000
Kyushu - Tohoku, Japan, May 28 - June 10, 2000

SELF-POTENTIAL VARIATION AT THE YANAIZU-NISHIYAMA GEOTHERMAL FIELD AND ITS INTERPRETATION BY THE NUMERICAL SIMULATION

[1)]Toshiyuki Tosha, Tsuneo Ishido, Nobuo Matsushima and Yuji Nishi
Geological Survey of Japan, 1-1-3 Higashi, Tsukuba, Ibaraki 305-8567, Japan
([1)] present address: New Energy and Industrial Technology Development Organization, 3-1-1 Higashi-Ikebukuro, Toshima, Tokyo 170-6028, Japan)

Key Words: self-potential, repeat surveys, postprocessor, numerical simulation

ABSTRACT

The Yanaizu-Nishiyama geothermal power plant commenced operating in May 1995. A positive self-potential (SP) anomaly was observed over the high temperature zones before the commencement of the fluid production. The positive SP anomaly disappeared on the profile in 1996, possibly owing to the development of the downward geothermal flow into the reservoir. Further surveys were carried out between May and September after 2 months' shut-in of all the production wells in 1998. The positive SP anomaly was again observed on the profile in May, but decreased with time after the re-start of production.

Numerical simulation was performed using a conceptual reservoir model and the SP variation was calculated. The model shows a positive SP anomaly above the high conductive vapour zone that is produced by the upward fluid flows for the natural-state condition. The production-induced flow becomes dominant during exploitation and the current sinks replace the positive sources of conduction current, resulting in the negative SP anomalies on the surface. The SP recovers substantially during the shut-in of the production wells. This is caused by the reduction in fluid flows from the vapour zone to the production zones. The SP decreases sharply after the re-start of production. The simulation reproduces the observed changes in SP at the Yanaizu-Nishiyama geothermal field.

1. INTRODUCTION

Geophysical surveys such as gravity, resistivity, microearthquake measurements at geothermal fields are carried out not only to find a geothermal reservoir in the exploration stage but to assess the environmental effects of power plants and/or to obtain the fundamental data for reservoir management. The SP method, which is conducted by mapping the natural electric field on the ground surface, is also carried out in geothermal fields both under natural and production states.

Positive SP anomalies were found to overlie high temperature upward flow zones in most of the geothermal fields (e.g. Ishido et al., 1990; Apostolopoulos et al., 1997) and also in volcanic regions (e.g. Hashimoto and Tanaka, 1995; Michel and Zlotnicki, 1998). The streaming potential generated by hydrothermal circulation is believed to be the most likely cause of the observed SP anomalies. In addition to SP anomalies in the natural state, changes in SP induced by production of fluids have been studied from repeated SP measurements in geothermal fields (e.g. Yasukawa et al., 1998). Electrokinetic coupling is also thought to be responsible for the production-induced changes in SP (e.g. Ishido et al., 1990). In this paper, the results of repeated SP surveys at the Yanaizu-Nishyama geothermal field, Japan, are presented and the SP variation with time is interpreted using a newly developed technique of numerical simulation (Ishido and Pritchett, 1999).

2. YANAIZU-NISHIYAMA GEOTHERMAL FIELD AND SP MEASUREMENT

2.1 Geological Background

The Yanaizu-Nishiyama (Okuaizu) geothermal field is located in Fukushima prefecture, *northeast* Honshu Island. Geological, geophysical and geochemical surveys have been carried out since 1974 for geothermal development. The Yanaizu-Nishiyama geothermal power plant commenced operation in May 1995 with 65MW capacity. Geology of this field is well investigated by many workers and is summarised in previous papers (e.g. Nitta et al, 1987, 1995; Mizugaki, 1999); the main production zones are composed of fractured Neogene formations along two NW-SE trending vertical faults, Chinoikezawa and Sarukurazawa faults (Fig. 1). These faults as well as the conjugate NE-SW trending systems are revealed by an alignment of hydrothermal manifestations, the distribution of resistivity, SP and soil gas anomalies and the locations of circulation losses in exploration wells (NEDO, 1985; Nitta et al., 1987, 1995; Sakai, 1987). The depth of the lost circulation points ranges from 1,000 to 2,600m below the surface, and highest temperatures recorded in wells ranges from 272 to 341 °C (Nitta et al., 1995). The reservoir is embedded in impermeable host rock formation.

The surface activities such as hot springs, fumaroles and vents are very limited. This relatively lower surface activity is interpreted as the results of the self-sealing of fractures by argillization and silicification (Nitta et al., 1995; Mizugaki, 1999). Weakly altered zones, which work as cap rocks of the geothermal system, are widely distributed with white clay minerals, smectitle, and the exposures of very intense alteration minerals along the faults. The extent of these altered zones was also indicated by the distribution of the high conductivity zones (more than 0.16S/m) delineated by an ELF-MT survey (Nitta et al., 1987). SP surveys were carried out in 1982-83 (12 years before the power plant start-up) to plot the SP distribution in the Yanaizu-Nishiyama area

(NEDO, 1985). A marked SP anomaly of positive polarity was found over high temperature zones, the amplitude of which was more than 110 mV, as occurred between the Sarukurazawa and the Oizawa faults, which is another NW-SE trending fault north of the Sarukurazawa fault (Fig. 1). This positive anomaly was interpreted as the result of the electrokinetic coupling caused by upward hydrothermal fluid flow (e.g. Ishido, 1989).

2.2 Repeat SP Surveys

We carried out the first repeat SP survey in November 1996, one and half years after the start-up of the Yanaizu-Nishiyama power plant. The survey line, about 12 km long, was chosen to pass through the positive SP anomaly reported by NEDO (Fig.1). The measurements were performed using a pair of non-polarizing Ag-AgCl electrodes placed every 100 m along the survey line. The closed loop offset was less than 25 mV, inferring that SP measurements had no serious error during the 12 km survey line. Fig. 2 shows the SP profile obtained from the 1996 survey together with that in 1982-83. As seen in the figure, a significant change took place between the profiles; the positive anomaly of more than 100 mV observed in 1982-83 had disappeared in 1996. Two sharp negative anomalies were found between 0.5 and 1 km along the profile in 1996 and are related to localized artificial effects (possibly caused by the construction with ferro-concrete for steam pipeline). There are, however, no steam pipelines close to the point "B" and the decrease in SP along the interval between the points "A" and "B" appears to be caused by production-induced changes in fluid flow pattern of the reservoir.

In order to confirm that the decrease in SP was induced by the change of the fluid flow, we repeated SP profiling along the survey line A-B (the location is shown in Fig.1) in 1998. Fig. 3 shows SP profiles obtained from four surveys carried out between May and September. The origin for each survey data was tentatively set at 2400 m in distance, which is thought far away from the SP variation region associated with the change of the geothermal reservoir. All of the production wells were shut in from March to May in 1998 for the maintenance of the Yanaizu-Nishiyama geothermal power plant. The survey in May was performed two days before the re-start of production after 2 months' shut-in and the surveys in June, July, and September were carried out one, two, and four months after the re-start, respectively. As shown in Fig. 3, the SP was positive in May in the interval between 1000 and 2400 m in distance, but decreased with time after the re-start of the power plant. The negative anomalies found at about 600 m and 1000 m in July and at 800 m in September are caused by the construction for steam pipelines. No steam pipelines were constructed in the interval between 1000 and 2400 m and the decrease is SP appears to be due to the changes of the fluid flow in the reservoir.

2.3 Continuous SP Measurements

A pair of non-polarizing Pb-$PbCl_2$ electrodes and a portable digital recorder were installed at about 1200m in distance to measure SP variation continuously. This continuous monitoring started in May and ended in November 1998. Two electrodes were set on about 100m apart along the survey line. Rainfall was also monitored at one of the reinjection bases in the Yanaizu-Nishiyama geothermal field.

Fig. 4. shows the SP variation with time. A positive polarity implies that the SP is increasing toward the point "B". The variation of rainfall in a 3 hours interval is also shown in the figure. The positive SP observed in May decreased to about 10 mV in November. The decrease was concordant with the repeat SP surveys shown in Fig. 3. The tendency of the decrease was, however, quite complex. Drastic drops of SP were found on several days which correlated with intense rainfalls. The relation between rainfall and SP is not clearly resolved. One possible reason is that rain water reduces the contact resistance. We are carrying out the other field experiment to solve the relation between rainfall and the sudden SP change.

3. NUMERICAL SIMULATION (EKP-Postprocessor)

In order to interpret the SP changes quantitatively, the "EKP-postprocessor" (Ishido and Pritchett, 1999) was applied to calculate the changes induced by fluid circulation in a geothermal reservoir. We first describe the EKP-postprocessor.

The fundamental equation that is solved by the "EKP postprocessor" is the following Poisson equation:

$$\nabla\cdot\mathbf{I}\mathrm{cond} = -\nabla\cdot\mathbf{I}\mathrm{drag} \qquad (1)$$

where **I**cond is a conduction current density caused by electric conduction and **I**drag is a drag (convection) current density caused by charges moved by fluid flow:

$$\mathbf{I}\mathrm{cond} = -Lee\,\nabla\phi$$

$$\mathbf{I}\mathrm{drag} = -Lev\,\nabla\xi$$

Here, *Lee* and *Lev* are the electrical conductivity of bulk fluid/rock composite and cross-coupling coefficient of electrokinetic effects respectively; $\nabla\phi$ and $\nabla\xi$ are the electric potential gradient and pore pressure gradient respectively.

The EKP postprocessor simulates electric potentials caused by subsurface fluid flow by a two-step process. First, it calculates the distribution of *Lev*, *Lee* and **I**drag from the results of the reservoir-simulation within the same spatial grid as used for the reservoir simulation calculation (called the RSV-grid hereafter). Next, the postprocessor calculates the electric potential (ϕ) distribution by solving Eq. 1 within a finite-difference grid, which is usually much greater in spatial extent than the RSV-grid (hereafter called the SP-grid).

Within the portion of the SP-grid overlapped by the RSV-grid, the distribution of electrical conductivity is calculated directly from the result in RSV-grid. Elsewhere within the SP-grid, the electrical conductivity distribution is user-specified and time-invariant. Ordinarily, boundary conditions on the potential are: zero normal gradient on the ground surface (upper surface) and zero potential along the bottom and vertical sides of the SP-grid. It is also possible to prescribe zero normal

gradient on all exterior surfaces of the SP-grid. Eq. 1 is solved numerically using a Gauss-Seidel iteration procedure which incorporates intermittent automatic optimization of the overrelaxation factor.

The drag current density within the RSV-grid is given by:

$$\mathbf{I}\text{drag} = - Lev\, \mathbf{M}_L \nu_L / k R_L \qquad (2)$$

where $\mathbf{M}_L$, ν_L and R_L are the mass flux density, kinematic viscosity and relative permeability of liquid phase, respectively, and k is the absolute permeability.

The coupling coefficient is computed based upon the capillary model described by Ishido and Mizutani (1981),

$$Lev = - \eta t^{-2} G\, Rev\, \varepsilon\, \zeta / \mu_L \qquad (3)$$

where η and t are the porosity and tortuosity of the porous medium; ε and μ_L are the dielectric permittivity and dynamic viscosity of the liquid phase; and ζ is the zeta potential, the potential across the electrical double layer. If ζ is negative (positive), positive (negative) charge is carried by the fluid flow **J**. The G and Rev factors are newly introduced: G (=< 1) is a correction factor for cases of very small hydraulic radius (comparable to the thickness of the electrical double layer) and Rev (=< 1) is a user-specified function of the liquid-phase saturation.

The zeta-potential in Eq. 3 is a function of temperature, pH and the concentration of 1:1 and 2:2 valent electrolyte in the solution, and is given by Eqs. 18, 20 and 21 of Ishido and Mizutani (1981) assuming the following empirical relation for the distance (Xs) between the solid surface and the slipping plane in the electrical double layer,

$$Xs\ (\text{meters}) = 3.4 \times 10^{-6}\, \mu_L\ (\text{pascal-seconds}) \qquad (4)$$

In the present version of the postprocessor, pH (ΔpH) must be supplied by the user as a function of position. The effects of Al^{+++} ion on ζ can also be taken into account. The dielectric permittivity ε is given as a function of temperature and pressure.

The electrical conductivity of the bulk fluid/rock composite (*Lee*) is calculated from the porosity and the conductivity of the rock matrix (σ_R) and the pore fluid (σ_F). Several types of "mixing law" are available in the postprocessor, such as Archie's law and the capillary model. The pore fluid conductivity is also calculated as the effective composite conductivity of the liquid, vapour and solid salt phases in the pores using one of several user-selected mixing laws. The liquid-phase conductivity is a function of temperature, pressure, and the concentrations of NaCl, KCl and $CaCl_2$ based on the formulation given by Olhoeft (1981).

4. DISCUSSION

4.1 Reservoir Model

The reservoir model used in the present study is a simple 3-D model as shown in Fig. 5; we try to incorporate major features of the Yanaizu-Nishiyama field described in Nitta et al. (1987) into this simple model. The high-permeable reservoir (A in Fig. 5), which represents the production zones along the nearly-vertical Sarukurazawa and Chinoikezawa faults, is overlain by the low-permeability altered caprock (C). Hot recharge water at temperature T_0 is assumed to enter the reservoir at the bottom with a mass flow rate M_0. A permeable peripheral formation (B) allows for lateral mass outflow. The rock (D) surrounding the reservoir is more permeable than the caprock, but less permeable so that conduction is the dominant mode of heat transfer. The hot recharge water boils as it rises through the system. In the upper part of the reservoir, a vapour/liquid two-phase zone is formed under the natural-state condition.

Rock properties of the formations shown in Fig. 5 are listed in Table 1. All exterior boundaries of the computational grid except the top surface and a part of the northwestern vertical surface, where the peripheral formation (B) intersects, are closed; pressure is maintained at 30 - 40 bars (30 bars at the northwestern end and increased linearly to 40 bars at the southeastern end) and temperature is at 80 °C along the top boundary (which is assumed to be located 500 m below the mean ground-surface level). The pressure at the depth of 1800 m along the northwestern boundary is maintained at 130 bars. Any "fresh water" which flows downward into the grid through the top surface contains a dilute tracer to permit its identification.

A source of high-temperature "magmatic water" (similarly tagged with a dilute tracer) was imposed on the southeastern bottom of reservoir (A) (T_0=350 °C, M_0=40 kg/s); the evolution of the hydrothermal convection system was then simulated using the STAR geothermal simulator (Pritchett, 1995). The system reached quasi-steady state after around 5000 years. The STAR simulator was also used to perform forecasts of the consequences of fluid production, starting from the natural-state model described above as the initial conditions. All boundary conditions and rock properties were the same as used to calculate the natural-state. Six hypothetical production wells (zones) were incorporated within the model. A constant total flowrate of 168 kg/s (equivalent to generate ~50 MW of electricity) was assumed to be withdrawn from the production wells. No reinjection was assumed in the present calculations. The distribution of vapour saturation after 1.25 years of field operation is shown in Fig. 6. The vapour zone expands about 600 m downward owing to the pressure decline caused by fluid production.

4.2 Simulation of SP Change

To forecast SP changes induced by the fluid production operations the computational/graphical EKP postprocessor for the STAR code was applied based on the exploitation model described above. For the self-potential calculations, the magmatic fluid is assumed to contain NaCl and Al^{+++}; the concentrations are proportional to the mass fraction of magmatic dilute tracer, and NaCl and Al^{+++} concentrations are 0.05 mol/L and $5\text{x}10^{-6}$ mol/L, respectively in the pure upflowing magmatic fluid intruding through the bottom. The fresh water is assumed to contain dilute NaCl (0.0017 mol/L). Rev in Eq.3 is set equal to 1 for all liquid saturations greater

than the residual saturation; this means **I**drag is not reduced for two-phase flow (containing vapour phase which cannot move charge) so long as the liquid phase flows. The postprocessor calculates *Lee*, *Lev* and **I**drag from the distributions of chemical composition and other results from the STAR simulation (such as temperature, pressure, liquid saturation and fluid mass flux) within the RSV-grid. Then the distribution of electric potential is calculated within the SP-grid.

The SP-grid extends over 8 km x 8 km in the horizontal direction, and 0 km < depth < 5 km in the vertical direction. Within the portion of the SP-grid overlapped by the RSV-grid, the distribution of electrical conductivity is obtained directly from RSV-grid values. The calculated representative bulk electrical conductivities of the fluid/rock composite (*Lee*) are ~0.1, ~0.05 and ~0.01 S/m for the formations (A), (B) and (D), respectively. *Lee* is calculated as ~0.3 S/m for the caprock region (C) by assuming high conductivity of the rock matrix. Elsewhere within the SP-grid, the electrical conductivity is given as 0.01 S/m except in a "high conductivity zone" connecting the caprock region in the RSV-grid and the ground surface. This high conductivity zone (0.3 S/m) was introduced to represent the shallow high conductivity anomalies revealed by the ELF/MT survey (NEDO, 1985; Nitta et al., 1987).

Fig. 7 shows the calculated potential distribution in a NW-SE vertical section for the natural-state condition. A positive SP anomaly is present above the "high conductivity vapour zone". This is produced by positive sources of conduction current:
$\nabla\cdot\mathbf{I}$cond (=$-\nabla\cdot\mathbf{I}$drag) has maximum around depth = 1 km and distance = 2.8 km. The ζ-potential changes from about –183 mV (at depth = 2.5 km) to –145 mV (at depth = 0.7 km) as the temperature decreases from 350 °C to 250 °C in the upward flow region. This brings about a large reduction in the drag current density along the upward flow path, resulting in positive charge accumulation.

The SP distributions during exploitation were calculated using the same parameter set as that used in the natural-state model. As seen Fig. 8, the flow pattern is dominated by production-induced flow. Sources and sinks of conduction current appear corresponding spatially to the feedpoints of the production wells and to the vapour/liquid two-phase zone (shown in Fig. 6), respectively. The current sinks replace the positive sources of conduction current around depth = 1 km and distance = 2.8 km which are present under the natural-state condition (compare Fig. 8 to Fig. 7), resulting in a SP anomaly of negative polarity on the ground surface.

Substantial production-induced expansion of the two-phase zone and increase in vapour saturation take place from the early stages of field operation (see Fig. 6). In and around the vapour zone, vigorous boiling occurs and significant fluid flows from the vapour zone to the feedpoints of production wells are produced. These flows of the liquid phase carry electric current (**I**drag) with them and bring about sinks and sources of conduction current corresponding spatially to the vapour zone and to the production zones, respectively.
Fig. 9 shows calculated change in ground-surface SP after fluid production (at distance = 2.2 km in Figs. 7. and 8). The production rate is maintained as 168 kg/s except the period from 450 to 540 days (during which the production rate is set to be zero). The SP decreases quickly to near zero during the first 3 months and continues to decrease afterwards in a more gradual rate. The SP recovers substantially toward positive side during the 3-month shut-in period (due to reduction in fluid flows from the vapour zone to the production zones), but decreases sharply after the re-start of production. The forecast presented here explains the observed changes in SP (shown in Figs. 2 and 3) at the Yanaizu-Nishiyama field.

5. CONCLUDING REMARKS

Several SP surveys were performed in 1996 and 1998 to monitor the hydrothermal circulation in the Yanaizu-Nishiyama geothermal field. The SP anomaly of positive polarity, which was found in the survey before the commencement of the geothermal power plant, decreased in amplitude for the survey in 1996. The amplitude of the positive anomaly increased after 2 months' shut-in of all the production wells in 1998. The repeat surveys and the continuous measurements of SP revealed the decrease of the positive anomaly in amplitude after the re-start of the production. The sudden decreases were also recorded in the continuous measurement of SP and were related to the amount of rainfall. The SP anomalies of the positive polarity are interpreted as the result of the electrokinetic coupling caused by upward hydrothermal fluid flow and the variation of the anomalies is due to the change of the hydrothermal circulation in the geothermal reservoir. Numerical simulation with the SP postprocessor shows the distribution of the hydrothermal flows and the electric potential and well explains the observed changes in SP at the Yanaizu-Nishiyama geothermal field. The SP surveys with a short interval and the continuous measurements are useful to constrain the parameters in the numerical simulation.

ACKNOWLEDGEMENTS

The present study was funded by MITI's New Sunshine Program, and the STAR simulations were run on the Cray-C90 supercomputer at the AIST-TACC computing complex in Tsukuba. Yanaizu-Nishiyama geothermal Co. is greatly acknowledged for their general courtesy during our field surveys. We also thank to NEDO for permitting us to use the rainfall data in this study.

REFERENCE

Apostplopoulos, G., Louis I. and Logios E. (1997). The self-potintial methos in the geothermal exploration of Greece, *Geothermics*, Vol. 62, pp.1715-1723.

Hashimoto, T. and Tanaka Y. (1995). A large self-potential anomaly on Unzen volcano, Simabara peninsula, Kyushu

island, Japan, *Geophy. Res. Lett*., Vol. 22, pp. 191-194.

Ishido, T.(1989). Self-potential Generation by Subsurface Water Flow Through Electrokinetic Coupling, In: *Detection of Subsurface Flow Phenomena*, G. P. Merkler et al.(Ed)., Lecture Notes in Earth Sciences, 27, Springer-Verlag, Berlin, pp.121-131.

Ishido, T. and Mizutani, H. (1981). Experimental and Theoretical Basis of Electrokinetic Phenomena in Rock-water Systems and its Applications to Geophysics, *J. Geophys. Res.*, Vol. 86, pp. 1763-1775.

Ishido, T. and Pritchett, J.W. (1999). Numerical simulation of electrokinetic potentials associated with subsurface fluid flow, submitted to *J. Geophys. Res*.

Ishido, T., Kikuchi, T., Yano, Y., Sugihara, M.,and Nakao, A. (1990). Hydrogeology inferred from the self-potential distribution, Kirishima geothermal field, Japan, *Geotherm. Res. Coun*., 14, 919-926, 1990.

Michel, S. and Zlotnicki, J. (1998). Self-potential and magnetic surveying of La Fournaise volcano (Reunion Island): Correlations with faulting, fluid circulation, and erution, *J. Geophys. Res.*, Vol. 103, pp. 17845-17857.

Mizugaki, M. (1999). Geological structure and volcanic history of the Yanaizu-Nishiyama (Okuaizu) geithernal field, Northeast Japan, submitted to *Geothermics*.

NEDO (New Energy Development Organization) (1985). *Geothermal Development Research Report, No. 8, Okuaizu region*, NEDO, Tokyo, 811pp. (in Japanese)

Nitta, T., Suga, S., Tsukagoshi, S., and Adachi, M. (1987). Geothermal resources in the Okuaizu, Tohoku district, Japan, *Chinetsu*, Vol. 24, pp. 26-56. (in Japanese with English abstract)

Nitta, T., Tsukagoshi, S., Adachi, M., and Seo, K. (1995). Exploration and development in the Okuaizu geothermal field, Japan, *Resource Geol*., Vol. 45, pp. 201-212.

Olhoeft, G.R. (1981). Electrical Properties of Rocks, In: *Physical Properties of Rocks and Minerals*, Y.S. Judd and R.F. Roy (Eds.), McGraw-Hill, New York, pp 257-329.

Pritchett, J.W. (1995). STAR: a Geothermal Reservoir Simulation System, In: *Proc. World Geothermal Congress,* Florence, pp.2959-2963.

Sakai, S. (1987). Applications of fingerprint geochemical technique for geothermal exploration, *Chinetsu-Energy*, Vol. 12, pp. 182-190. (in Japanese)

Yasukawa, K., Matsushima, N., Kikuchi, T., Ishido, T., Kuwano, T., Suzuki, I., and Takahashi, M. (1998). Transient of Self-potential distribution at the Nigorikawa area, *Abst. 1998 Ann. Meet. Geotherm. Res. Soc. Jpn.*, pp3-23. (in Japanese)

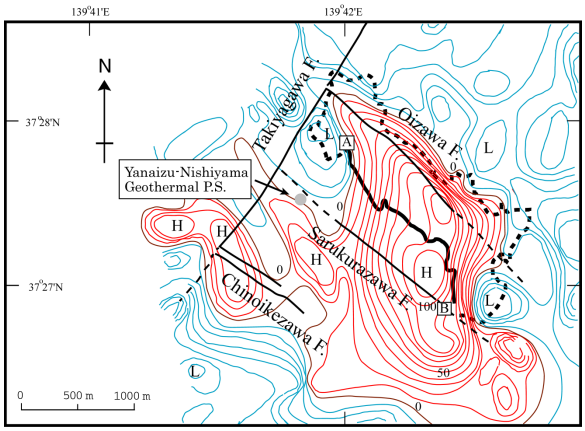

Fig. 1 Fault system and SP distribution at the 1982-83 survey in the yanaizu-Nishiyama area

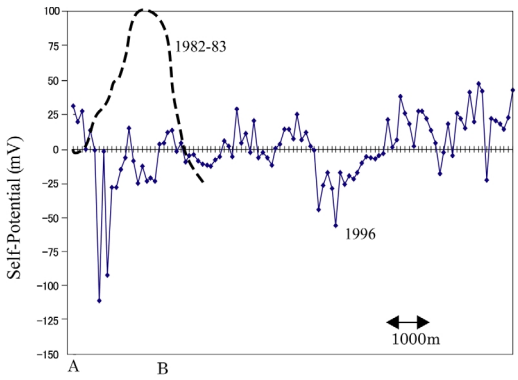

Fig. 2 SP profile along the survey line shown in Fig. 1. The survey was carried out in 1996 at 1.5 years after the commencement of the production. The dashed line shows the SP profile in 1982-83, 12 years before the power plant start-up.

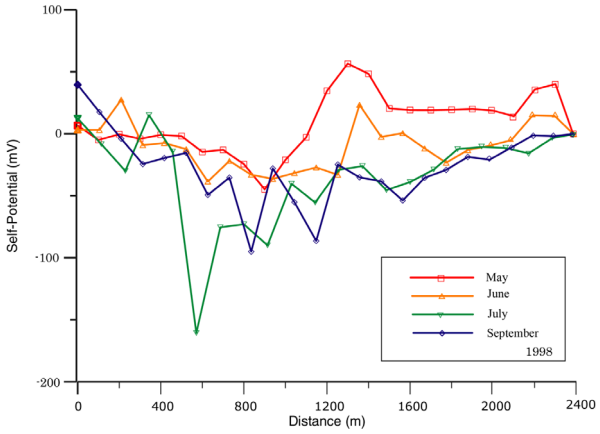

Fig. 3. SP profiles at the repeat surveys from May to September, 1998.

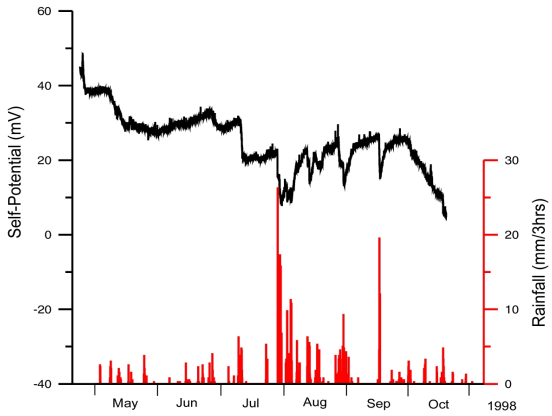

Fig. 4. The continuous SP record and the rainfall in 1998.

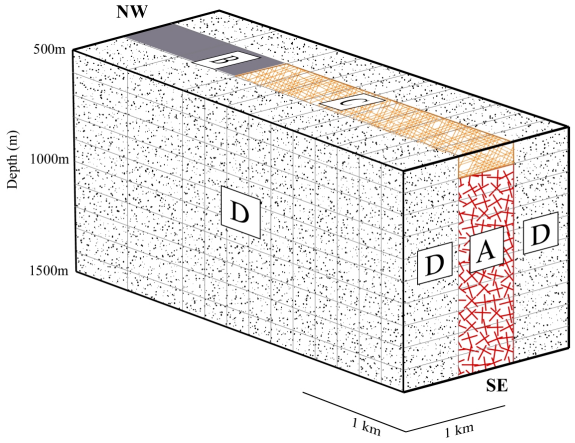

Fig. 5. A conceptual 3-D model for the Yanaizu-Nishiyama field. Rock properties are listed in Table 1.

Rock Type	X	Y	Z
A (reservoir)	100	10	10
B (peripheral)	30	10	10
C (Caprock)	0.1	0.1	0.1
D (Wall)	3	3	3

Table 1. Permeability in each formation in milli-darcy

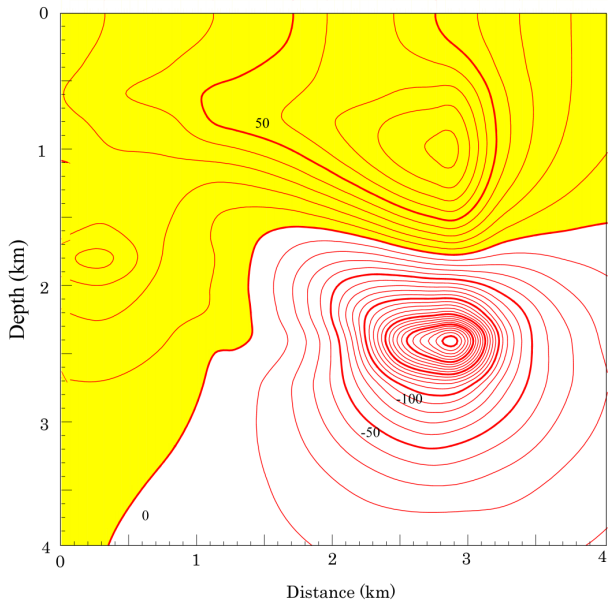

Fig. 7. The distribution of the electric potential calculated in a NW-SE vertical section for the natural stage. Yellow (Gray) zone indicates the anomaly of the positive polarity

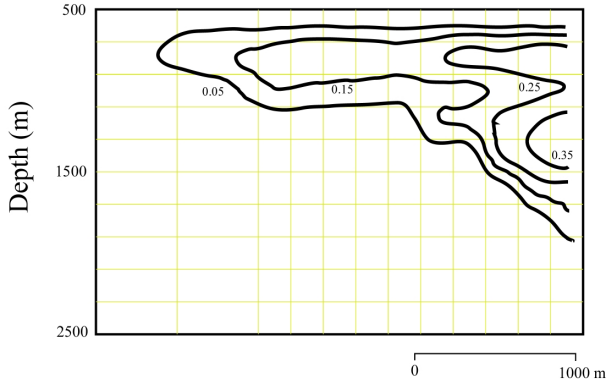

Fig. 6. The distribution of vapour saturation after 1.25 years of field operation

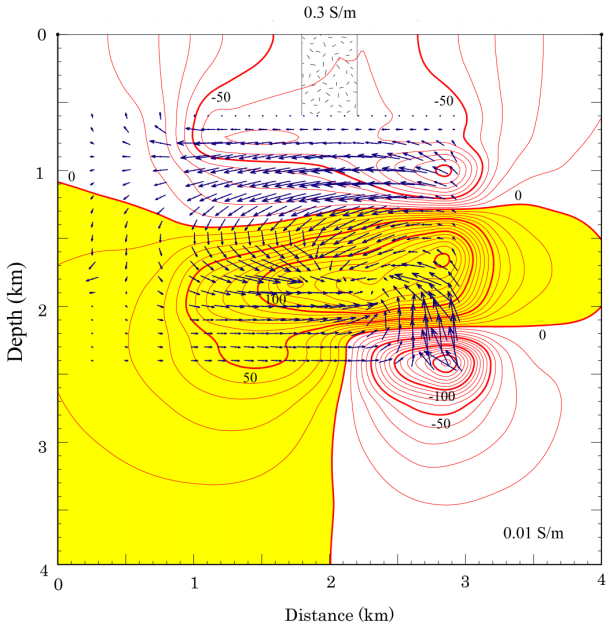

Fig. 8. The flow pattern and the SP distribution during the exploration in the same vertical section as in Fig. 7

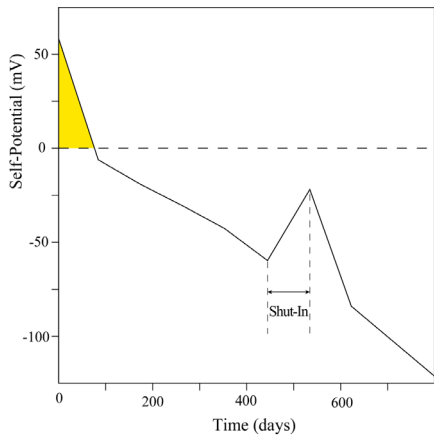

Fig. 9. The SP variation with time after the production of the fluid.